

Supplementary Material for:
Marginal Bayesian Semiparametric Modeling of Mismeasured
Multivariate Interval-Censored Data

LI LI, ALEJANDRO JARA, MARÍA JOSÉ GARCÍA-ZATTERA,
AND TIMOTHY E. HANSON

April 24, 2018

¹Li Li is Assistant Professor, Department of Mathematics and Statistics, The University of New Mexico, Albuquerque, NM 87131, USA (E-mail: llis@unm.edu), María José García-Zattera is Adjunct Assistant Professor, Department of Statistics, Pontificia Universidad Católica de Chile, Casilla 306, Correo 22, Santiago, Chile (E-mail: mjgarcia@uc.cl). Alejandro Jara is Associate Professor, Department of Statistics, Pontificia Universidad Católica de Chile, Casilla 306, Correo 22, Santiago, Chile (E-mail: atjara@uc.cl). Timothy E. Hanson is Senior Principal Statistician, Medtronic, Inc., 710 Medtronic Parkway N.E., Minneapolis, MN 55432 USA (E-mail: tim.hanson2@medtronic.com).

Appendix A: Illustration of the data generating mechanism

Figure 1 illustrates the observed data generating mechanism.

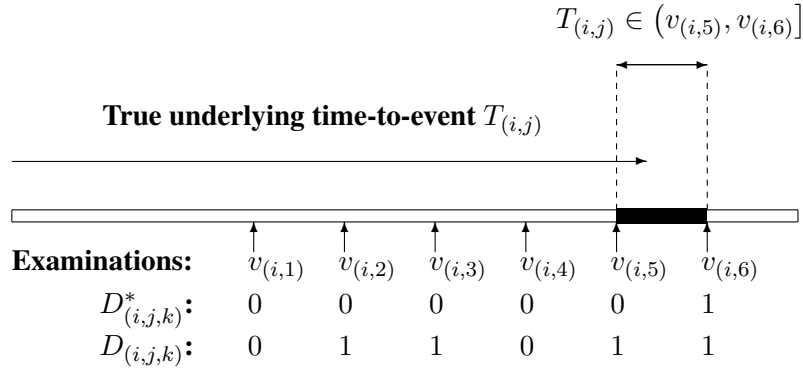


Figure 1: Illustration of the data generating mechanism. In a regular interval-censored data context, the time-to-event $T_{(i,j)}$ is unobserved but is known with certainty to lie in the interval $(v_{(i,5)}, v_{(i,6)}]$. In this case, the observed data can be represented by the binary variables $D_{(i,j,k)}^*$ indicating whether evaluation indicates that the event has occurred by time $v_{(i,k)}$ ($D_{(i,j,k)}^* = 1$), or not ($D_{(i,j,k)}^* = 0$), $k = 1, \dots, 6$. Under misclassification, however, an error-corrupted version of the $D_{(i,j,k)}^*$'s are observed, denoted by $D_{(i,j,k)}$, $k = 1, \dots, 6$.

Appendix B: MCMC sampling under an unrestricted correlation matrix

The MCMC algorithm for sampling the parameters from the joint posterior of the marginal models under an unrestricted correlation matrix is outlined here. Treating \mathbf{T} as latent variables, the augmented likelihood function is given by

$$L(\boldsymbol{\alpha}, \boldsymbol{\eta}, \boldsymbol{\beta}, \boldsymbol{\rho}, F_0, \mathbf{T}|\mathbf{D}) = \prod_{i=1}^N \prod_{j=1}^J \prod_{k=1}^{K_i+1} A_{(i,j,k)}^{I(T_{(i,j)} \in (v_{(i,k-1)}, v_{(i,k)}])} \quad (\text{B.1})$$

$$\times \prod_{i=1}^N \left\{ \frac{1}{(\sqrt{2\pi})^J |\mathbf{R}_\rho|^{1/2}} \exp \left\{ -\frac{1}{2} \mathbf{Z}'_i \mathbf{R}_\rho^{-1} \mathbf{Z}_i \right\} \prod_{j=1}^J \frac{f_{\mathbf{x}_{(i,j)}}(T_{(i,j)})}{\phi(\Phi^{-1}(F_{\mathbf{x}_{(i,j)}}(T_{(i,j)})))} \right\}$$

where $\mathbf{Z}_i = (Z_{(i,1)}, \dots, Z_{(i,J)})$ and $Z_{(i,j)} = \Phi^{-1}(F_{\mathbf{x}_{(i,j)}}(T_{(i,j)}))$.

1. **Sampling $T_{(i,j)}$:** we sample $Z_{(i,j)}$ first and then set $T_{(i,j)} = F_{\mathbf{x}_{(i,j)}}^{-1}(\Phi(Z_{(i,j)}))$. Denote $\mathbf{R}_{(j,j)}$ as the (j, j) th element of \mathbf{R}_ρ , $\mathbf{R}_{(j,-j)}$ as the j th column of \mathbf{R}_ρ without the j -th element, $\mathbf{R}_{(-j,-j)}$ as the sub-matrix of \mathbf{R}_ρ without the j -th row and column, and $\mathbf{Z}_{(i,-j)}$ as the sampled latent vector \mathbf{Z}_i without the j th element. The conditional distribution of $Z_{(i,j)}$ given data, latent survival times, and model parameters is proportional to:

$$\prod_{k=1}^{K_i+1} A_{(i,j,k)}^{I(Z_{(i,j)} \in (\Phi^{-1}(F_{\mathbf{x}_{(i,j)}}(v_{(i,k-1)})), \Phi^{-1}(F_{\mathbf{x}_{(i,j)}}(v_{(i,k)}))))} N(Z_{(i,j)}, \mu_{(i,j)}, \sigma_{(i,j)}^2), \quad (\text{B.2})$$

where

$$\mu_{(i,j)} = \mathbf{z}'_{(i,-j)} \mathbf{R}_{(-j,-j)}^{-1} \mathbf{R}_{(j,-j)}; \quad \sigma_{(i,j)}^2 = \mathbf{R}_{(j,j)} - \mathbf{R}'_{(j,-j)} \mathbf{R}_{(-j,-j)}^{-1} \mathbf{R}_{(j,-j)}. \quad (\text{B.3})$$

The conditional distribution implied in Expression B.2 is a mixture of truncated Normal distributions with weights

$$\pi_k = A_{(i,j,k)} \left(\Phi \left(\frac{\Phi^{-1}(F_{\mathbf{x}_{(i,j)}}(v_{(i,k)})) - \mu_{(i,j)}}{\sigma_{(i,j)}} \right) - \Phi \left(\frac{\Phi^{-1}(F_{\mathbf{x}_{(i,j)}}(v_{(i,k-1)})) - \mu_{(i,j)}}{\sigma_{(i,j)}} \right) \right),$$

where $k = 1, \dots, K_i + 1$. To draw a sample from the mixture, one approach is to firstly draw a sample from a multinomial distribution of size one and $\pi_1, \dots, \pi_{K_i+1}$ as probabilities for $K_i + 1$ classes; then sample $Z_{(i,j)}$ from the selected truncated Normal distribution component.

2. **Sampling of $\boldsymbol{\alpha}$:** we set $\boldsymbol{\varphi} = \text{logit}(\boldsymbol{\alpha})$ and considered a logistic-Normal approximation to the original beta prior. The conditional posterior of $\boldsymbol{\varphi}$ is proportional to

$$\prod_{i=1}^N \prod_{j=1}^J \prod_{k=1}^{K_i+1} A_{(i,j,k)}^{I(T_{(i,j)} \in (v_{(i,k-1)}, v_{(i,k)}])} N(\boldsymbol{\varphi}; \mathbf{m}_\varphi, \mathbf{V}_\varphi) \quad (\text{B.4})$$

$$\times \prod_{j=1}^J \prod_{q=1}^Q \mathbb{I}(\eta_{(q,j)}, \alpha_{(q,j)}) \{(\eta_{(q,j)}, \alpha_{(q,j)}): \eta_{(q,j)} + \alpha_{(q,j)} > 1\}$$

We update φ in a single block using the adaptive Metropolis-Hasting algorithm described by Haario et al. (2001).

3. **Sampling of η :** we set $\phi = \text{logit}(\eta)$ and considered a logistic-Normal approximation to the original beta prior. The conditional posterior of ϕ is proportional to

$$\begin{aligned} & \prod_{i=1}^N \prod_{j=1}^J \prod_{k=1}^{K_i+1} A_{(i,j,k)}^{I(T_{(i,j)} \in (v_{(i,k-1)}, v_{(i,k)}])} N(\phi; \mathbf{m}_\phi, \mathbf{V}_\phi) \\ & \times \prod_{j=1}^J \prod_{q=1}^Q \mathbb{I}(\eta_{(q,j)}, \alpha_{(q,j)}) \{(\eta_{(q,j)}, \alpha_{(q,j)}): \eta_{(q,j)} + \alpha_{(q,j)} > 1\}. \end{aligned} \quad (\text{B.5})$$

We update ϕ in a single block using the adaptive Metropolis-Hasting algorithm.

4. **Sampling of β, λ, θ :** The conditional posterior is proportional to

$$\begin{aligned} & \prod_{i=1}^N \left\{ \frac{1}{(\sqrt{2\pi})^J |\mathbf{R}_\rho|^{\frac{1}{2}}} \exp \left\{ -\frac{1}{2} \mathbf{Z}'_i \mathbf{R}_\rho^{-1} \mathbf{Z}_i \right\} \prod_{j=1}^J \frac{f_{\mathbf{x}_{(i,j)}}(T_{(i,j)})}{\phi(\Phi^{-1}(F_{\mathbf{x}_{(i,j)}}(T_{(i,j)})))} \right\} \\ & \times N(\beta; \mathbf{m}_\beta, \mathbf{V}_\beta) N(\theta; \mathbf{m}_\theta, \mathbf{V}_\theta) \prod_{\epsilon} N(\lambda_{\epsilon 0}; 0, 2/[c_j^2]). \end{aligned} \quad (\text{B.6})$$

We update β, λ, θ in three blocks using the adaptive Metropolis-Hasting algorithm.

5. **Sampling of \mathbf{R}_ρ :** Adopting the uniform prior on correlation matrix proposed by Liu and Daniels (2006), the conditional posterior is proportional to

$$\begin{aligned} & \prod_{i=1}^N \frac{1}{(\sqrt{2\pi})^J |\mathbf{R}_\rho|^{\frac{1}{2}}} \exp \left\{ -\frac{1}{2} \mathbf{Z}'_i \mathbf{R}_\rho^{-1} \mathbf{Z}_i \right\} \\ & \times I \{ R_{(j,k)}; R_{(j,k)} = 1(j=k), |R_{(j,k)}| < 1(j \neq k) \text{ and } \mathbf{R}_\rho \text{ is positive definite} \}, \end{aligned} \quad (\text{B.7})$$

$$\times I \{ R_{(j,k)}; R_{(j,k)} = 1(j=k), |R_{(j,k)}| < 1(j \neq k) \text{ and } \mathbf{R}_\rho \text{ is positive definite} \}, \quad (\text{B.8})$$

where $I(\cdot)$ is an indicator function. To sample \mathbf{R}_ρ , first construct a diagonal matrix

$$\mathbf{U} = \text{diag} \left(\frac{1}{\sqrt{\sum_{i=1}^N Z_{(i,1)}^2}}, \dots, \frac{1}{\sqrt{\sum_{i=1}^N Z_{(i,J)}^2}} \right)$$

and let $\mathbf{W} = \mathbf{U}(\sum_{i=1}^N \mathbf{Z}_i \mathbf{Z}'_i) \mathbf{U}$. Sample a symmetric matrix Σ^* from a Wishart distribution that is proportional to

$$|\Sigma^*|^{-\frac{N+J+1}{2}} \exp \left\{ -\frac{1}{2} \text{tr}(\mathbf{W} \Sigma^{*-1}) \right\}.$$

Then standardize Σ^* to obtain a candidate correlation matrix \mathbf{R}^* . Finally accept \mathbf{R}^* with probability

$$\min \left\{ 1, \exp \left\{ \frac{J+1}{2} \left(\log(|\mathbf{R}^*|) - \log(|\mathbf{R}_\rho^{\text{old}}|) \right) \right\} \right\}.$$

Appendix C: True time-to-event models

Figure 2 displays the true time-to-event marginal models employed in the simulation study.

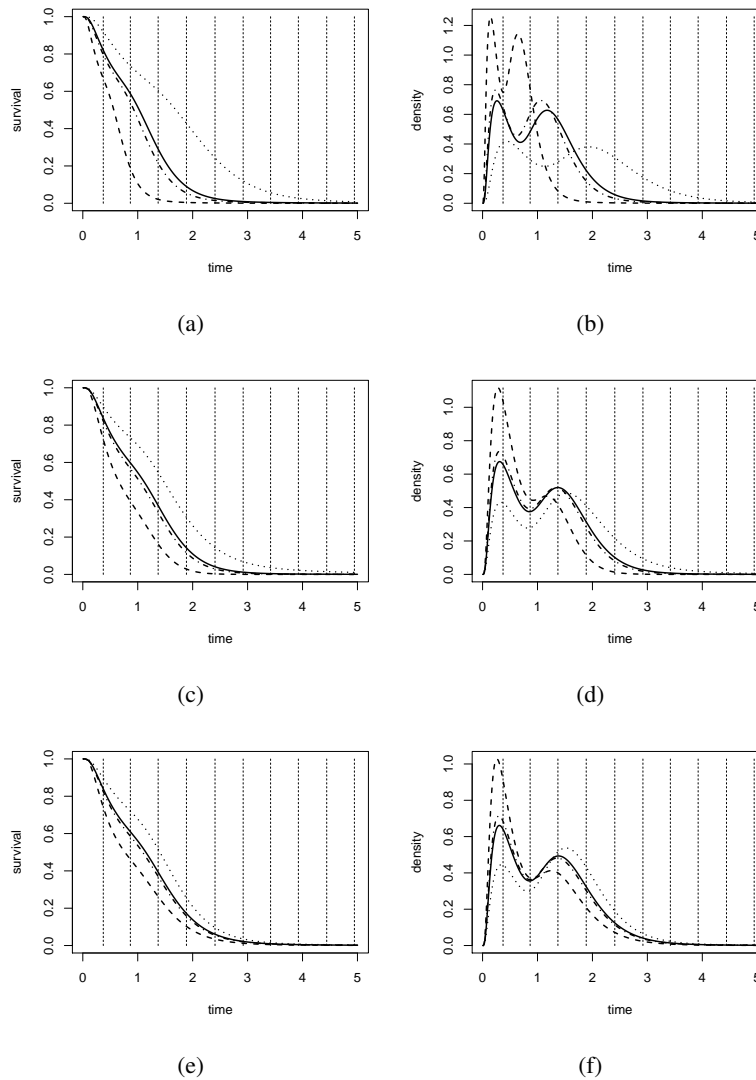


Figure 2: Simulated data. True time-to-event marginal models. The results are shown for $\mathbf{x} = (0, 0.2)$, $\mathbf{x} = (0, 0.8)$, $\mathbf{x} = (1, 0.2)$, and $\mathbf{x} = (1, 0.8)$, as solid, dashed, dotted, and dotdashed lines, respectively. Panels (a) and (b) display the true survival and density function under the AFT model, respectively. Panels (c) and (d) display the true survival and density function under the PH model, respectively. Panels (e) and (f) display the true survival and density function under the PO model, respectively. In every plot, the expected visit times are displayed as vertical dashed lines.

Appendix D: Computation of CPO under an unrestricted correlation matrix

Due to the sampling of many latent survival times for the marginal model assuming an unrestricted correlation matrix, the calculation of log-pseudo marginal likelihood (LPML) becomes challenging. In this section, we present a marginalized method to compute LPML. Specifically, let

$$\begin{aligned}
 p_{M_i}(\mathbf{D}_i | \mathbf{D}^{[-i]}) &= \left\{ E_{\boldsymbol{\alpha}, \boldsymbol{\eta}, \boldsymbol{\beta}, \boldsymbol{\rho}, F_0} \left(\frac{1}{p(\mathbf{D}_i | \boldsymbol{\alpha}, \boldsymbol{\eta}, \boldsymbol{\beta}, \boldsymbol{\rho}, F_0)} \right) \right\}^{-1}, \\
 p(\mathbf{D}_i | \boldsymbol{\alpha}, \boldsymbol{\eta}, \boldsymbol{\beta}, \boldsymbol{\rho}, F_0) &= \int \prod_{j=1}^J \prod_{k=1}^{K_i+1} A_{(i,j,k)}^{I(Z_{(i,j)} \in (\Phi^{-1}(F_{\mathbf{x}_{(i,j)}}(v_{(i,k-1)})), \Phi^{-1}(F_{\mathbf{x}_{(i,j)}}(v_{(i,k)}))))} \times \\
 &\quad \frac{1}{(\sqrt{2\pi})^J |\mathbf{R}_\rho|^{\frac{1}{2}}} \exp \left\{ -\frac{1}{2} \mathbf{Z}'_i \mathbf{R}_\rho^{-1} \mathbf{Z}_i \right\} d\mathbf{Z}_i
 \end{aligned} \tag{D.1}$$

which can be computed as

$$\sum_{k_1=1}^{K_i+1} \cdots \sum_{k_J=1}^{K_i+1} A_{(i,1,k_1)} \cdots A_{(i,J,k_J)} \int_{B_{k_1, \dots, k_J}} \frac{1}{(\sqrt{2\pi})^J |\mathbf{R}_\rho|^{\frac{1}{2}}} \exp \left\{ -\frac{1}{2} \mathbf{Z}'_i \mathbf{R}_\rho^{-1} \mathbf{Z}_i \right\} d\mathbf{Z}_i$$

with $B_{k_1, \dots, k_J} = \prod_{j=1}^J I(Z_{(i,j)} \in (\Phi^{-1}(F_{\mathbf{x}_{(i,j)}}(v_{(i,k_j-1)})), \Phi^{-1}(F_{\mathbf{x}_{(i,j)}}(v_{(i,k_j)}))))$. The multivariate Normal integration was done using the method by Genz (1992).

Appendix E: Additional results for the simulation study

Additional results for simulation Scenarios II and III described in the main paper are presented here. For both Scenarios, simulated data were generated assuming an unstructured correlation matrix. In Scenario II, common effects of the predictors across teeth and common examiner misclassification parameters are assumed. In Scenario III, tooth-specific effects of predictors and tooth-specific misclassification parameters are assumed.

Tables 1 and 2 show the means (across simulations), biases, and the MSE of the posterior mean of the parameters from the different versions of the proposed semiparametric model, from the different time-to-event modeling assumptions under Scenarios II and III.

Table 1: Simulated data - Scenario II. True value, Monte Carlo mean, bias, and mean square error (MSE) of the posterior mean of the time-to-event model parameters. The results are presented for different group sample sizes (N) and true underlying time-to-event model assumptions (PH, AFT and PO).

N	Parameter	True Value	True Marginal Model								
			PH			AFT			PO		
			Mean	Bias	MSE	Mean	Bias	MSE	Mean	Bias	MSE
100	β_1	-0.5	-0.473	0.027	0.016505	-0.491	0.009	0.004539	-0.500	0.000	0.041289
	β_2	1.0	1.063	0.063	0.050181	1.032	0.032	0.016347	1.088	0.088	0.136902
	ρ_{12}	0.4	0.361	0.039	0.020798	0.367	0.033	0.022377	0.357	0.043	0.019549
	ρ_{13}	0.2	0.189	0.011	0.018648	0.176	0.024	0.023040	0.179	0.021	0.017456
	ρ_{14}	0.1	0.076	0.024	0.024810	0.085	0.015	0.026248	0.094	0.006	0.022528
	ρ_{23}	0.4	0.365	0.035	0.019990	0.369	0.031	0.022734	0.368	0.032	0.019196
	ρ_{24}	0.2	0.174	0.026	0.022542	0.190	0.010	0.024272	0.197	0.003	0.017102
	ρ_{34}	0.4	0.354	0.046	0.022821	0.376	0.024	0.024665	0.393	0.007	0.020039
200	β_1	-0.5	-0.479	0.021	0.007488	-0.488	0.012	0.002363	-0.482	0.018	0.019553
	β_2	1.0	1.037	0.037	0.025492	1.019	0.019	0.009418	1.042	0.042	0.053257
	ρ_{12}	0.4	0.384	0.016	0.008797	0.391	0.009	0.009426	0.378	0.022	0.009230
	ρ_{13}	0.2	0.184	0.016	0.010405	0.196	0.004	0.011627	0.188	0.012	0.009849
	ρ_{14}	0.1	0.078	0.022	0.010247	0.102	0.002	0.012681	0.097	0.003	0.008349
	ρ_{23}	0.4	0.395	0.005	0.008845	0.392	0.008	0.009315	0.385	0.015	0.009341
	ρ_{24}	0.2	0.178	0.022	0.010631	0.182	0.018	0.011394	0.188	0.012	0.009515
	ρ_{34}	0.4	0.381	0.019	0.010591	0.384	0.016	0.009510	0.384	0.016	0.008976
300	β_1	-0.5	-0.487	0.013	0.004348	-0.492	0.008	0.002004	-0.490	0.010	0.014274
	β_2	1.0	1.030	0.030	0.015923	1.025	0.025	0.006501	1.040	0.040	0.041429
	ρ_{12}	0.4	0.389	0.011	0.005735	0.395	0.005	0.007147	0.396	0.004	0.005862
	ρ_{13}	0.2	0.186	0.014	0.006507	0.193	0.007	0.006814	0.191	0.009	0.005891
	ρ_{14}	0.1	0.091	0.009	0.007155	0.086	0.014	0.007554	0.091	0.009	0.007324
	ρ_{23}	0.4	0.396	0.004	0.005652	0.390	0.010	0.006847	0.387	0.013	0.005830
	ρ_{24}	0.2	0.194	0.006	0.006548	0.190	0.010	0.006888	0.191	0.009	0.006210
	ρ_{34}	0.4	0.385	0.015	0.006639	0.391	0.009	0.006273	0.395	0.005	0.005517

Table 2: Simulated data - Scenario III. True value, and Monte Carlo mean, bias and mean square error (MSE) of the posterior mean of the regression parameters and correlation parameters. The results are presented for different sample sizes (N) and true underlying time-to-event model assumptions (PH, AFT and PO).

N	Parameter	True Value	True Marginal Model								
			PH			AFT			PO		
			Mean	Bias	MSE	Mean	Bias	MSE	Mean	Bias	MSE
100	β_{11}	-0.5	-0.453	0.047	0.052804	-0.488	0.012	0.018214	-0.479	0.021	0.148512
	β_{12}	1.0	1.139	0.139	0.160027	1.043	0.043	0.040074	1.130	0.130	0.324347
	β_{21}	-0.5	-0.450	0.050	0.065516	-0.492	0.008	0.015348	-0.486	0.014	0.143227
	β_{22}	1.0	1.110	0.110	0.159068	1.058	0.058	0.034575	1.111	0.111	0.336543
	β_{31}	-0.5	-0.461	0.039	0.045043	-0.475	0.025	0.014182	-0.507	0.007	0.142655
	β_{32}	1.0	1.104	0.104	0.128577	1.027	0.027	0.030831	1.125	0.125	0.278845
	β_{41}	-0.5	-0.451	0.049	0.059357	-0.480	0.020	0.017863	-0.456	0.044	0.157969
	β_{42}	1.0	1.112	0.112	0.173157	1.031	0.031	0.037882	1.114	0.114	0.302049
	ρ_{12}	0.4	0.352	0.048	0.020166	0.371	0.029	0.019470	0.366	0.034	0.017096
	ρ_{13}	0.2	0.176	0.024	0.020765	0.180	0.020	0.025473	0.174	0.026	0.018000
	ρ_{14}	0.1	0.091	0.009	0.026377	0.094	0.006	0.023228	0.083	0.017	0.026876
	ρ_{23}	0.4	0.366	0.034	0.022830	0.363	0.037	0.021904	0.378	0.022	0.020136
	ρ_{24}	0.2	0.175	0.025	0.024778	0.183	0.017	0.024109	0.186	0.014	0.017117
	ρ_{34}	0.4	0.389	0.011	0.021484	0.378	0.022	0.022318	0.395	0.005	0.021220
200	β_{11}	-0.5	-0.459	0.041	0.022895	-0.489	0.011	0.008049	-0.494	0.006	0.072939
	β_{12}	1.0	1.064	0.064	0.049636	1.036	0.036	0.017577	1.057	0.057	0.148518
	β_{21}	-0.5	-0.464	0.036	0.024494	-0.484	0.016	0.007498	-0.498	0.002	0.065049
	β_{22}	1.0	1.055	0.055	0.054149	1.016	0.016	0.019826	1.087	0.087	0.145125
	β_{31}	-0.5	-0.475	0.025	0.022203	-0.486	0.014	0.008480	-0.498	0.002	0.065970
	β_{32}	1.0	1.081	0.081	0.061905	1.030	0.030	0.017146	1.085	0.085	0.141871
	β_{41}	-0.5	-0.477	0.023	0.022130	-0.501	0.001	0.007529	-0.502	0.002	0.067757
	β_{42}	1.0	1.084	0.084	0.063142	1.046	0.046	0.018449	1.082	0.082	0.133330
	ρ_{12}	0.4	0.379	0.021	0.008272	0.382	0.018	0.012161	0.394	0.006	0.008976
	ρ_{13}	0.2	0.190	0.010	0.010154	0.174	0.026	0.012472	0.181	0.019	0.010987
	ρ_{14}	0.1	0.092	0.008	0.010512	0.091	0.009	0.012590	0.089	0.011	0.010385
	ρ_{23}	0.4	0.389	0.011	0.009871	0.381	0.019	0.010644	0.387	0.013	0.008932
	ρ_{24}	0.2	0.185	0.015	0.010379	0.191	0.009	0.012668	0.198	0.002	0.010002
	ρ_{34}	0.4	0.387	0.013	0.009115	0.381	0.019	0.010732	0.395	0.005	0.009102
300	β_{11}	-0.5	-0.477	0.023	0.015354	-0.484	0.016	0.005904	-0.492	0.008	0.042405
	β_{12}	1.0	1.071	0.071	0.037589	1.027	0.027	0.012296	1.054	0.054	0.088331
	β_{21}	-0.5	-0.474	0.026	0.015872	-0.494	0.006	0.004687	-0.489	0.011	0.043090
	β_{22}	1.0	1.060	0.060	0.038792	1.023	0.023	0.010127	1.051	0.051	0.087701
	β_{31}	-0.5	-0.482	0.018	0.014880	-0.491	0.009	0.004585	-0.492	0.008	0.042525
	β_{32}	1.0	1.064	0.064	0.037120	1.021	0.021	0.012032	1.060	0.060	0.086226
	β_{41}	-0.5	-0.470	0.030	0.018752	-0.490	0.010	0.005643	-0.495	0.005	0.038679
	β_{42}	1.0	1.054	0.054	0.036311	1.031	0.031	0.011642	1.047	0.047	0.094696
	ρ_{12}	0.4	0.381	0.019	0.006450	0.380	0.020	0.007847	0.388	0.012	0.006988
	ρ_{13}	0.2	0.193	0.007	0.006683	0.188	0.012	0.007525	0.188	0.012	0.006794
	ρ_{14}	0.1	0.092	0.008	0.006830	0.099	0.001	0.007609	0.097	0.003	0.006369
	ρ_{23}	0.4	0.391	0.009	0.005820	0.389	0.011	0.006692	0.388	0.012	0.005893
	ρ_{24}	0.2	0.186	0.014	0.006508	0.197	0.003	0.007408	0.195	0.005	0.006740
	ρ_{34}	0.4	0.387	0.013	0.005738	0.384	0.016	0.006279	0.392	0.008	0.006905

Figure 3 shows true value, mean of the posterior mean across simulations, and 95% confidence intervals for the sensitivity and specificity of each examiner under Scenario II.

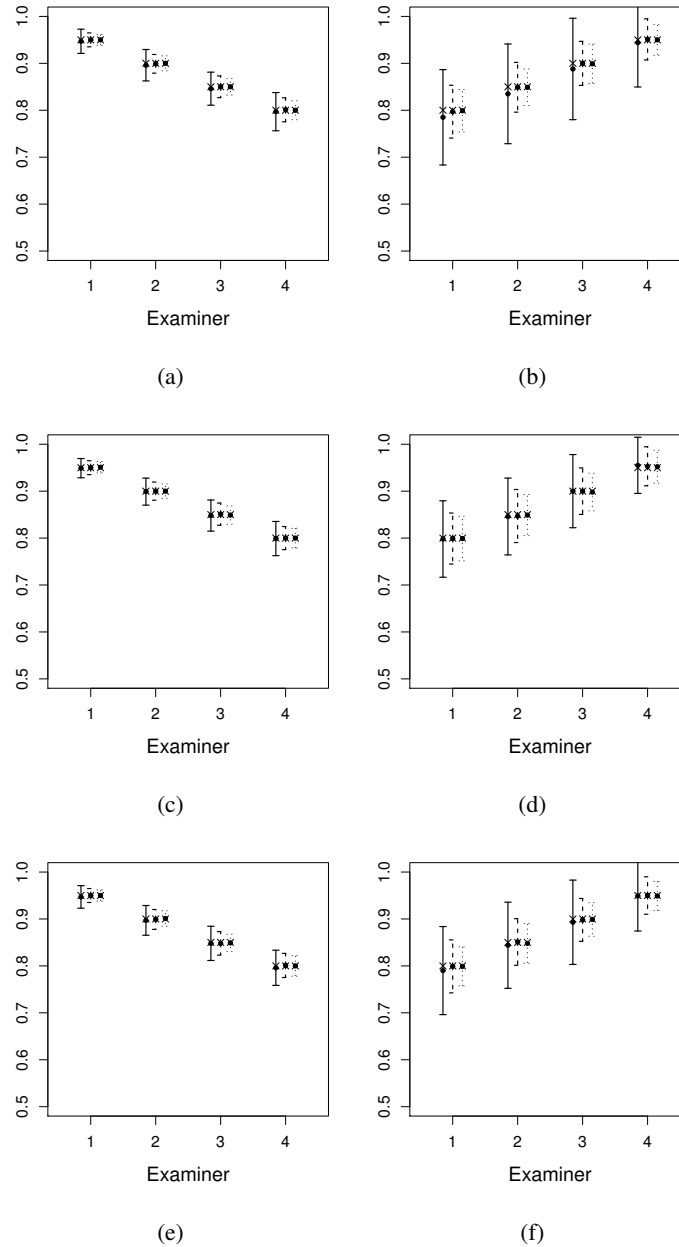


Figure 3: Simulated data - Scenario II. True value (\times), mean of the posterior mean across simulations (\bullet) $\pm 1.96 \times \sqrt{\text{MSE}}$ for the sensitivity and specificity of each examiner. The results for $N = 100$, $N = 200$ and $N = 300$ are displayed as solid, dashed and dotted lines, respectively. Panels (a) and (b), (c) and (d), and (e) and (f) display the results under a true PH, AFT and PO marginal time-to-event model, respectively. Panels (a), (c) and (e) display the results for the sensitivity. Panels (b), (d) and (f) display the results for the specificity.

Figure 4 shows true value, mean of the posterior mean across simulations, and 95% confidence intervals for the sensitivity and specificity of each examiner for tooth 1, under Scenario III.

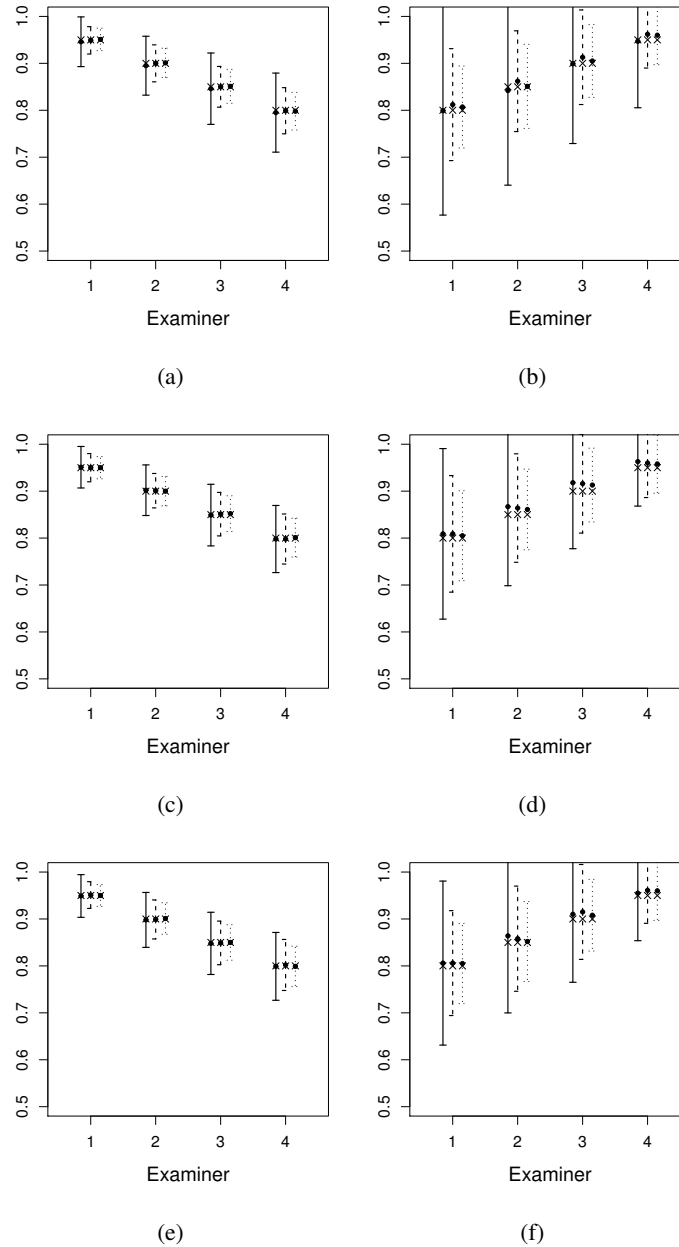


Figure 4: Simulated data - Scenario III. True value (\times), mean of the posterior mean across simulations (\bullet) $\pm 1.96 \times \sqrt{\text{MSE}}$ for the sensitivity and specificity of each examiner on tooth 1. The results for $N = 100$, $N = 200$ and $N = 300$ are displayed as solid, dashed and dotted lines, respectively. Panels (a) and (b), (c) and (d), and (e) and (f) display the results under a true PH, AFT and PO marginal time-to-event model, respectively. Panels (a), (c) and (e) display the results for the sensitivity. Panels (b), (d) and (f) display the results for the specificity.

Figure 5 shows true value, mean of the posterior mean across simulations, and 95% confidence intervals for the sensitivity and specificity of each examiner for tooth 2, under Scenario III.

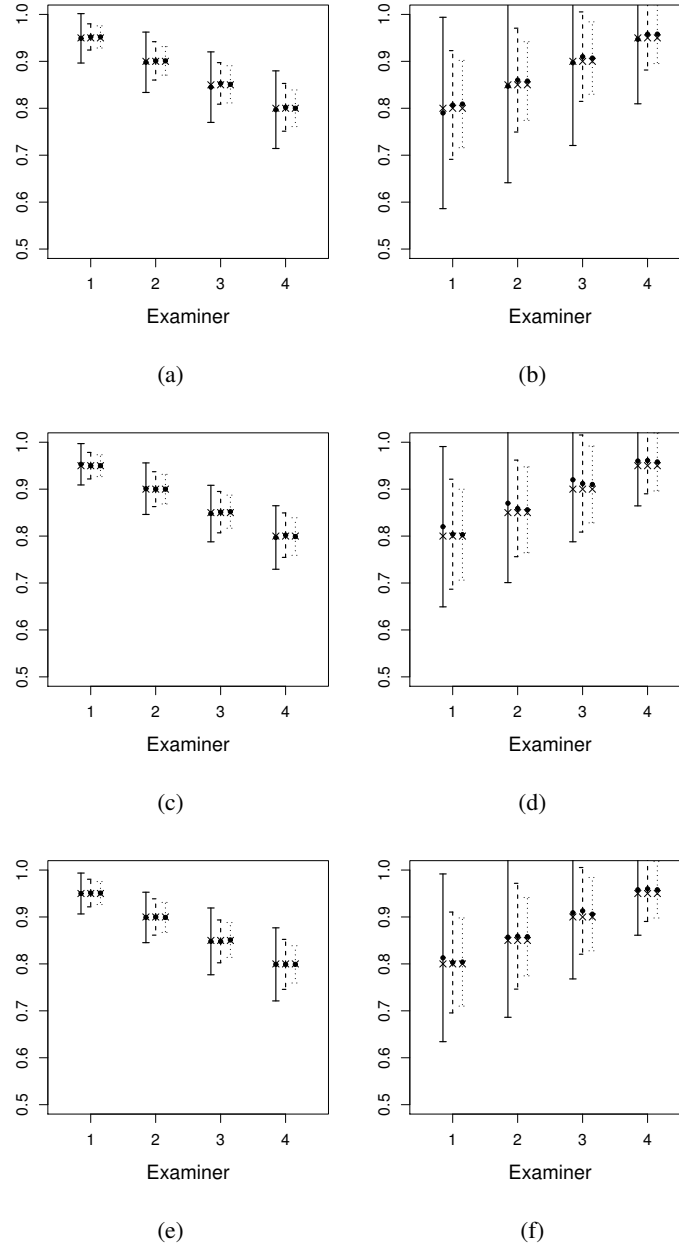


Figure 5: Simulated data - Scenario III. True value (\times), mean of the posterior mean across simulations (\bullet) $\pm 1.96 \times \sqrt{\text{MSE}}$ for the sensitivity and specificity of each examiner on tooth 2. The results for $N = 100$, $N = 200$ and $N = 300$ are displayed as solid, dashed and dotted lines, respectively. Panels (a) and (b), (c) and (d), and (e) and (f) display the results under a true PH, AFT and PO marginal time-to-event model, respectively. Panels (a), (c) and (e) display the results for the sensitivity. Panels (b), (d) and (f) display the results for the specificity.

Figure 6 shows true value, mean of the posterior mean across simulations, and 95% confidence intervals for the sensitivity and specificity of each examiner for tooth 3, under Scenario III.

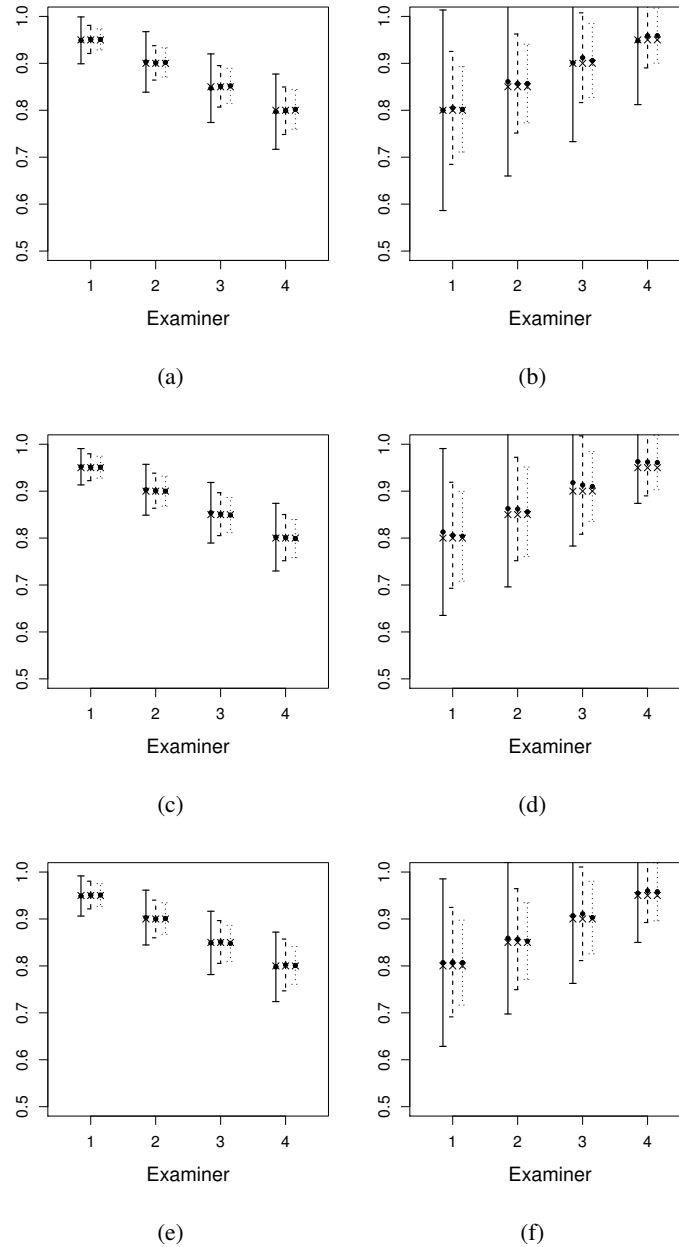


Figure 6: Simulated data - Scenario III. True value (\times), mean of the posterior mean across simulations (\bullet) $\pm 1.96 \times \sqrt{\text{MSE}}$ for the sensitivity and specificity of each examiner on tooth 3. The results for $N = 100$, $N = 200$ and $N = 300$ are displayed as solid, dashed and dotted lines, respectively. Panels (a) and (b), (c) and (d), and (e) and (f) display the results under a true PH, AFT and PO marginal time-to-event model, respectively. Panels (a), (c) and (e) display the results for the sensitivity. Panels (b), (d) and (f) display the results for the specificity.

Figure 7 shows true value, mean of the posterior mean across simulations, and 95% confidence intervals for the sensitivity and specificity of each examiner for tooth 4, under Scenario III.

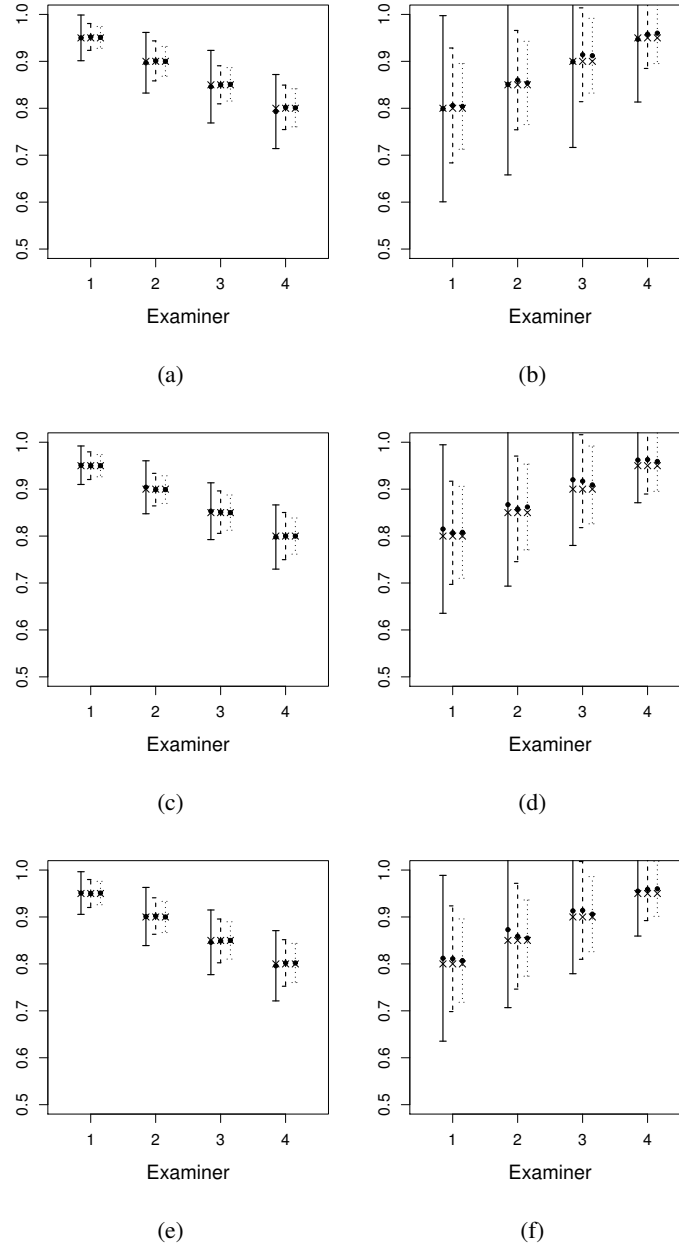


Figure 7: Simulated data - Scenario III. True value (\times), mean of the posterior mean across simulations (\bullet) $\pm 1.96 \times \sqrt{\text{MSE}}$ for the sensitivity and specificity of each examiner on tooth 4. The results for $N = 100$, $N = 200$ and $N = 300$ are displayed as solid, dashed and dotted lines, respectively. Panels (a) and (b), (c) and (d), and (e) and (f) display the results under a true PH, AFT and PO marginal time-to-event model, respectively. Panels (a), (c) and (e) display the results for the sensitivity. Panels (b), (d) and (f) display the results for the specificity.

Scenario IV

Finally, in Scenario IV we consider a variation of Scenario I, where a different baseline distribution is assumed by considering $F_0(\cdot) = 0.5 \times \text{LN}(\cdot \mid 1, 0.2^2) + 0.5 \times \text{LN}(\cdot \mid 2, 0.2^2)$. In this case, we set $\mathbf{x}_{(i,j)} = (x_{(i,j,1)}, x_{(i,j,2)})$, assume a compound symmetry correlation matrix and common effects of the predictors across teeth, and set $\rho = 0.2$ and $\beta_j = (-0.5, 1)$, for every j . The true time-to-events were interval-censored by simulating the “visit” times for each subject. We considered $K_i = 10$. The time between the consecutive visits, $\nu_{i,k} - \nu_{i,k-1}$, was drawn from an $\text{LN}(0, 0.2^2)$ distribution. We assumed that the assessment of the occurrence of the event was performed by $Q = 4$ examiners, allocated randomly to each subject and visit. We further assumed common misclassification parameters for each examiner across variables and set $\alpha = (0.95, 0.90, 0.85, 0.80)$ and $\eta = (0.80, 0.85, 0.90, 0.95)$.

The true time-to-event marginal models are shown in Figure 8.

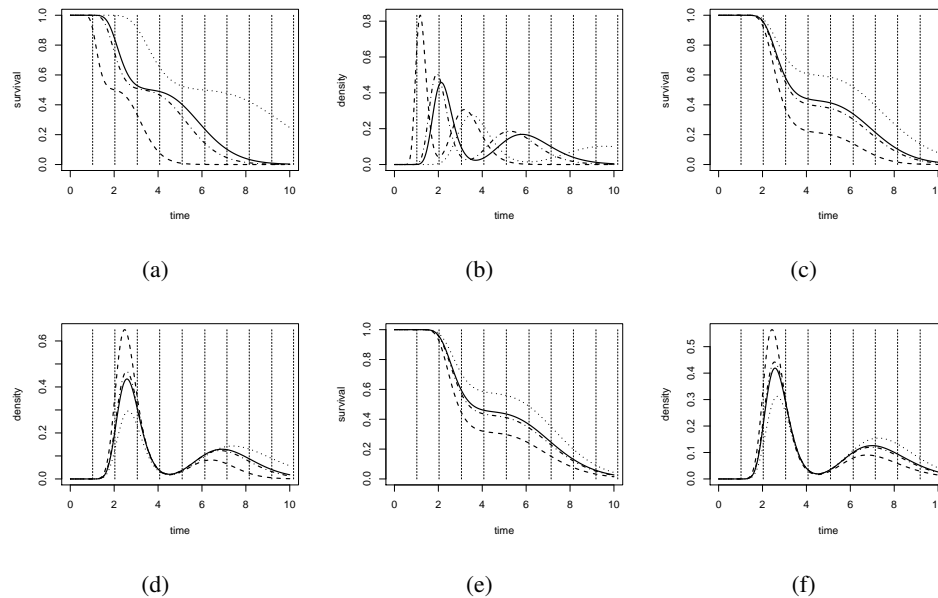


Figure 8: Simulated data. True time-to-event marginal models. The results are shown for $\mathbf{x} = (0, 0.2)$, $\mathbf{x} = (0, 0.8)$, $\mathbf{x} = (1, 0.2)$, and $\mathbf{x} = (1, 0.8)$, as solid, dashed, dotted, and dotdashed lines, respectively. Panels (a) and (b) display the true survival and density function under the AFT model, respectively. Panels (c) and (d) display the true survival and density function under the PH model, respectively. Panels (e) and (f) display the true survival and density function under the PO model, respectively. In every plot, the expected visit times are displayed as vertical dashed lines.

Table 3 shows the means, across simulations, the biases and the MSE of the posterior mean of the parameters from the different versions of the semiparametric model, under the different time-to-event modeling assumptions under Scenario VI.

Table 3: Simulated data - Scenario IV. True value, and Monte Carlo mean, bias and mean square error (MSE) of the posterior mean of the time-to-event model parameters. The results are presented for different sample sizes (N) and true underlying time-to-event model assumptions (PH, AFT and PO). In this table, the same true time-to-event model is assumed to simulate and to fit the data.

N	Parameter	True Value	True Marginal Model								
			PH			AFT			PO		
			Mean	Bias	MSE	Mean	Bias	MSE	Mean	Bias	MSE
100	β_1	-0.5	-0.505	0.005	0.015222	-0.506	0.006	0.001371	-0.507	0.007	0.042744
	β_2	1.0	0.946	0.054	0.047723	1.003	0.003	0.005475	0.904	0.096	0.125597
	ρ	0.2	0.241	0.041	0.005439	0.247	0.047	0.005916	0.231	0.031	0.004579
200	β_1	-0.5	-0.504	0.004	0.007014	-0.501	0.001	0.000818	-0.515	0.015	0.020779
	β_2	1.0	0.953	0.047	0.026582	1.001	0.001	0.002674	0.930	0.070	0.063445
	ρ	0.2	0.215	0.015	0.002415	0.222	0.022	0.002771	0.219	0.019	0.002110
300	β_1	-0.5	-0.508	0.008	0.005521	-0.498	0.002	0.000465	-0.508	0.008	0.012752
	β_2	1.0	0.972	0.028	0.012058	1.005	0.005	0.001385	0.971	0.029	0.036824
	ρ	0.2	0.213	0.013	0.001508	0.213	0.013	0.001367	0.207	0.007	0.001364

Figure 9 shows the results regarding bias and MSE for the misclassification parameters under Scenario IV.

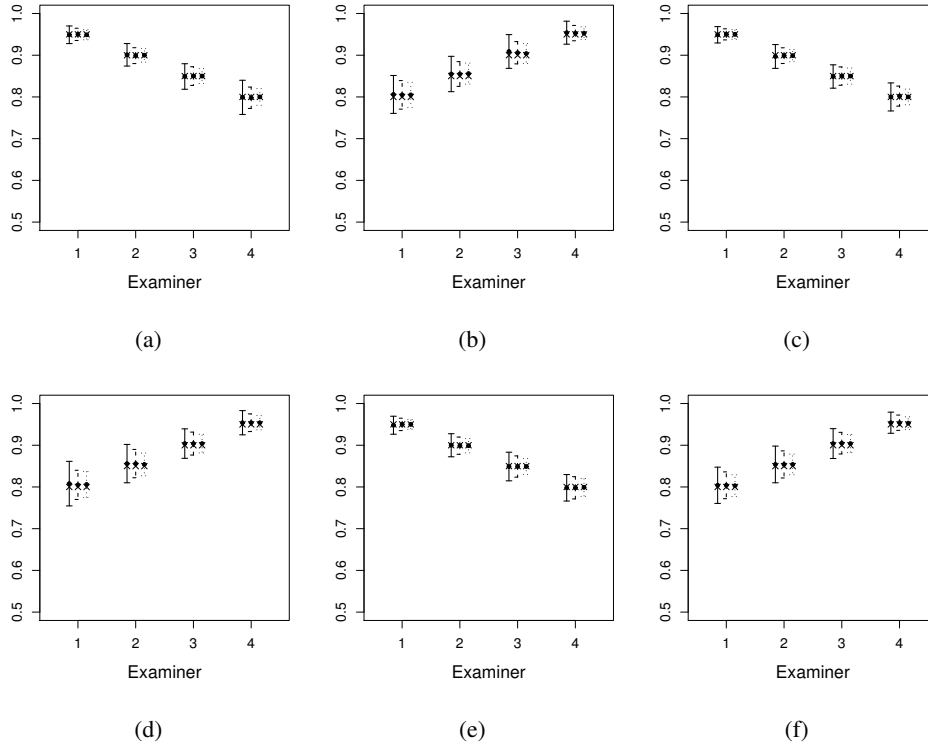


Figure 9: Simulated data - Scenario IV: True value (\times), mean of the posterior mean across simulations (\bullet) $\pm 1.96 \times \sqrt{\text{MSE}}$ for the sensitivity and specificity of each examiner. The results for $N = 100$, $N = 200$ and $N = 300$ are displayed as solid, dashed and dotted lines, respectively. Panels (a) and (b), (c) and (d), and (e) and (f) display the results under a true PH, AFT and PO marginal time-to-event model, respectively. Panels (a), (c) and (e) display the results for the sensitivity. Panels (b), (d) and (f) display the results for the specificity.

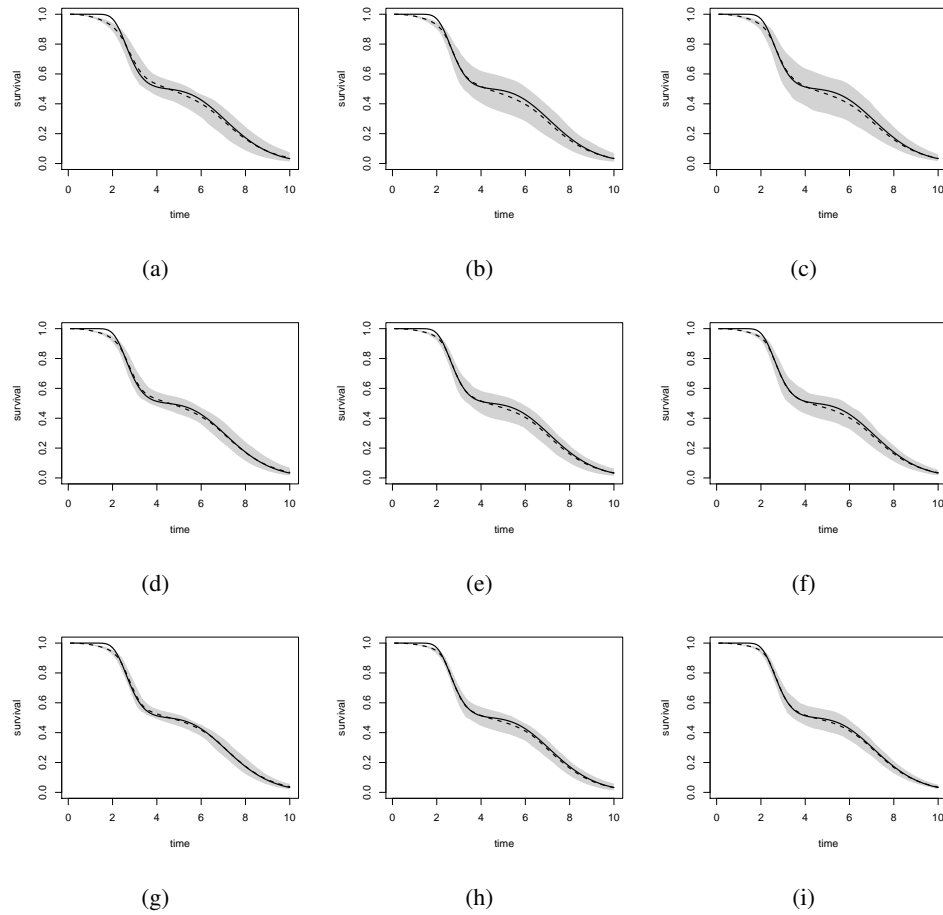


Figure 10: Simulated data - Scenario IV. Mean across simulations of the posterior mean of the baseline survival function (dashed line), point-wise 95% confidence region (shaded). The true survival function is represented as a solid line. Panels (a), (b), and (c) display the results for $N = 100$ under a true PH, AFT and PO marginal model, respectively. Panels (d), (e), and (f) display the results for $N = 200$ under a true PH, AFT and PO marginal model, respectively. Panels (g), (h), and (i) display the results for $N = 300$ under a true PH, AFT and PO marginal model, respectively.

Table 4 and Figure 11 show the results for the naive analysis assuming no misclassification.

Table 4: Simulated data - Scenario IV. True value, and Monte Carlo mean, bias and mean square error (MSE) of the posterior mean of the time-to-event model parameters for different sample sizes. The results are presented for naive fitting of AFT, PO, and PH models.

N	Parameter	Fitted Model									
		True Value	PH			AFT			PO		
			Mean	Bias	MSE	Mean	Bias	MSE	Mean	Bias	MSE
100	β_1	-0.5	-0.327	0.173	0.039359	-0.454	0.046	0.003335	-0.342	0.158	0.053627
	β_2	1.0	0.750	0.250	0.093899	0.958	0.042	0.006723	0.663	0.337	0.197527
	ρ	0.2	0.119	0.081	0.007892	0.129	0.071	0.006825	0.114	0.086	0.008747
200	β_1	-0.5	-0.333	0.167	0.032680	-0.459	0.041	0.002348	-0.325	0.175	0.045937
	β_2	1.0	0.752	0.248	0.075768	0.964	0.036	0.003882	0.660	0.340	0.163351
	ρ	0.2	0.097	0.103	0.011629	0.108	0.092	0.009553	0.099	0.101	0.011090
300	β_1	-0.5	-0.334	0.166	0.030542	-0.459	0.041	0.002132	-0.324	0.176	0.042325
	β_2	1.0	0.763	0.237	0.065705	0.961	0.039	0.003310	0.686	0.314	0.128289
	ρ	0.2	0.093	0.107	0.012189	0.100	0.100	0.010820	0.094	0.106	0.011887

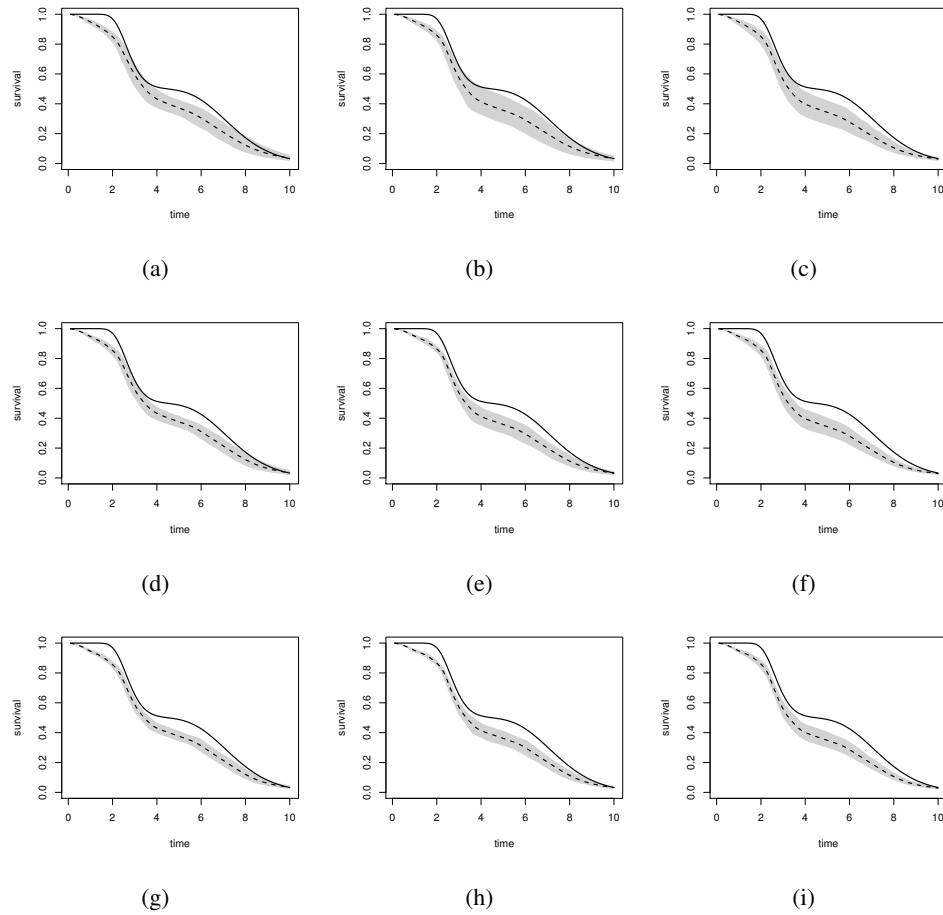


Figure 11: Simulated data - Scenario IV. Mean across simulations of the posterior mean of the baseline survival function (dashed line), point-wise 95% confidence region (shaded) under the a naive analysis ignoring the misclassification process. The true survival function is represented as a solid line. Panels (a), (b), and (c) display the results for $N = 100$ under a true PH, AFT and PO marginal model, respectively. Panels (d), (e), and (f) display the results for $N = 200$ under a true PH, AFT and PO marginal model, respectively. Panels (g), (h), and (i) display the results for $N = 300$ under a true PH, AFT and PO marginal model, respectively.

Appendix F: Simulation results for inferences under an incorrect model and misclassification

In this section we illustrate the effect of using a wrong probability survival model for making inferences. Under this situation, it is expected to obtain incorrect inferences associated with parameters with different interpretations (the regression coefficient) and with parameters highly influenced by the model assumptions (the marginal survival functions, which varies as a function of predictors in different ways under the different models). However, parameters with a common interpretation (the association structure and misclassification parameters) should fare better.

For an illustration of these points, we have also implemented the extended hazard (EH) version of the proposed model (Chen and Jewell, 2001; Li, Hanson and Zhang, 2015). The EH model assumes the following relationship among the baseline survival distribution, the predictors, and the marginal survival distributions:

$$1 - F_{\mathbf{x}_{(i,j)}}(t) = \left(1 - F_0 \left(\exp\{\mathbf{x}'_{(i,j)}\boldsymbol{\zeta}\}t\right)\right)^{\exp\{\mathbf{x}'_{(i,j)}\boldsymbol{\beta}\}}.$$

The EH model is a more flexible survival model, including AFT and PH as special cases. As expected, based on the results shown in the original version of the paper, when the EH assumption holds the LPML correctly selects the true underlying time-to-event regression assumption and accurate estimates of the model parameters are obtained when the EH model is fit. As an illustration, Table 5 shows the results for the EH version of the proposed model when the data is generated from a EH model. The results in this table are for $N = 100$ and under the same simulation settings considered in the original version of the paper. In this case, the LPML selects the correct EH model 92.5% of the time.

As expected, when wrong models are fit to data arising from an EH model, misleading inferences are observed for parameters stemming from models with incorrect interpretations depending on the survival assumption, but precise estimators are obtained for parameters with a common interpretation across models. Table 6 shows the results of the model parameter estimation under different wrong models, when the data is generated from an EH model. Note that in this table the bias and MSE for the regression coefficients are obtained by comparing the regression coefficients under the PH, AFT and PO versions of the model, with the different set of coefficients under the true EH model.

Figure 12 and 13 display the results for the estimation of the marginal survival functions for different

Table 5: Simulated data - EH model - $N = 100$: True value, and Monte Carlo mean, bias and mean square error (MSE) of the posterior mean of the model parameters.

Parameter	True value	Mean	Bias	MSE
β_1	-0.50	-0.490	0.010	0.020350
β_2	1.00	1.018	0.018	0.061392
ζ_1	0.00	0.003	0.003	0.003585
ζ_2	0.50	0.492	0.008	0.011928
ρ	0.20	0.233	0.033	0.004431
α_1	0.95	0.949	0.001	0.000087
α_2	0.90	0.901	0.001	0.000161
α_3	0.85	0.848	0.002	0.000261
α_4	0.80	0.799	0.001	0.000326
η_1	0.80	0.809	0.009	0.000757
η_2	0.85	0.857	0.007	0.000557
η_3	0.90	0.908	0.008	0.000473
η_4	0.95	0.957	0.007	0.000270

Table 6: Simulated data - EH model - $N = 100$: True value, and Monte Carlo mean, bias and mean square error (MSE) of the posterior mean of the time-to-event model parameters. The results are presented for different incorrect time-to-event model assumptions (PH, AFT and PO).

Parameter	True Value	Fitted Model								
		PH			AFT			PO		
		Mean	Bias	MSE	Mean	Bias	MSE	Mean	Bias	MSE
β_1	-0.50	-0.484	0.016	0.016195	-0.135	0.365	0.135470	-0.784	0.284	0.126568
β_2	1.00	1.583	0.583	0.388940	0.646	0.354	0.130915	2.279	1.279	1.767286
ζ_1	0.00	-0.484	0.484	0.250442	-0.135	0.135	0.020302	-0.784	0.784	0.660914
ζ_2	0.50	1.583	1.083	1.221916	0.646	0.146	0.027063	2.279	1.779	3.296515
ρ	0.20	0.233	0.033	0.004431	0.231	0.031	0.004155	0.229	0.029	0.004255
α_1	0.95	0.949	0.001	0.000090	0.950	0.000	0.000090	0.949	0.001	0.000090
α_2	0.90	0.900	0.000	0.000165	0.901	0.001	0.000162	0.900	0.000	0.000162
α_3	0.85	0.848	0.002	0.000268	0.849	0.001	0.000258	0.848	0.002	0.000275
α_4	0.80	0.799	0.001	0.000330	0.800	0.000	0.000323	0.799	0.001	0.000332
η_1	0.80	0.809	0.009	0.000775	0.807	0.007	0.000731	0.808	0.008	0.000764
η_2	0.85	0.857	0.007	0.000575	0.857	0.007	0.000551	0.857	0.007	0.000581
η_3	0.90	0.908	0.008	0.000484	0.907	0.007	0.000474	0.907	0.007	0.000480
η_4	0.95	0.957	0.007	0.000272	0.957	0.007	0.000271	0.956	0.006	0.000276

combinations of the predictors.

The results illustrate that it is expected to observe wrong inferences associated with parameters with different interpretations (the regression coefficients) and with parameters highly influenced by the model

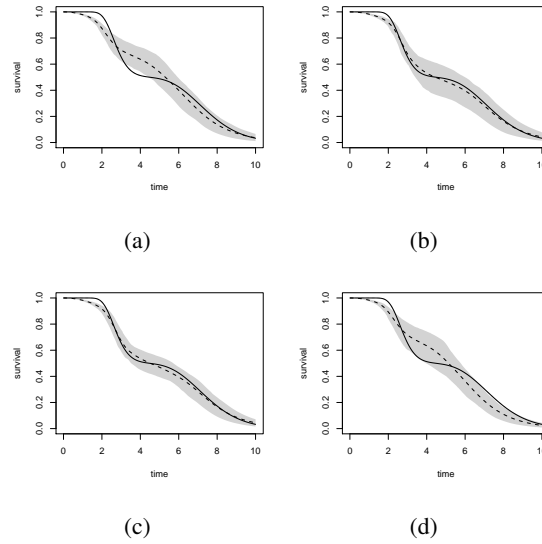


Figure 12: Simulated data - EH model - $N = 100$: True survival function (continuous line), posterior mean (dotted line) and 95% pointwise credible regions (gray area) for marginal survival function for $\mathbf{x} = (0, 0)$. Panels (a), (b), (c), and (d) present the results under a PH, EH, AFT, and PO underlying time-to-event model assumption, respectively.

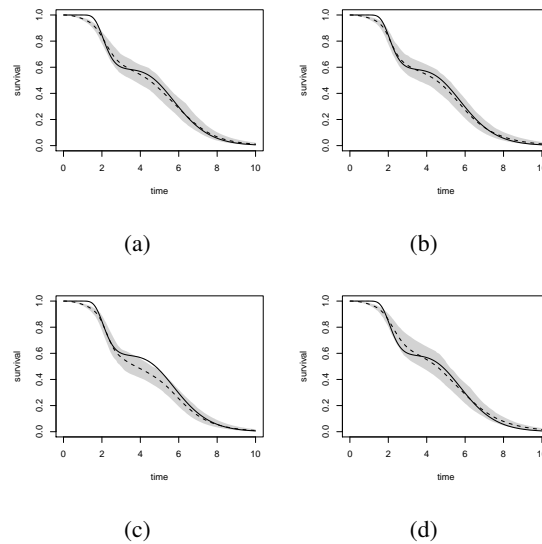


Figure 13: Simulated data - EH model - $N = 100$: True survival function (continuous line), posterior mean (dotted line) and 95% pointwise credible regions (gray area) for marginal survival function for $\mathbf{x} = (1.0, 0.5)$. Panels (a), (b), (c), and (d) present the results under a PH, EH, AFT, and PO underlying time-to-event model assumption, respectively.

assumptions (the marginal survival functions, which varies as a function of predictors in different ways under the different models). However, no or little effects are expected on parameters with a common

interpretation (the association structure and misclassification parameters).

Appendix G: Spatial trend for the apparent prevalence of CE

Figure 14 shows the apparent prevalence of caries experience (CE) for the different geographical locations of the schools, for the different years of examination.

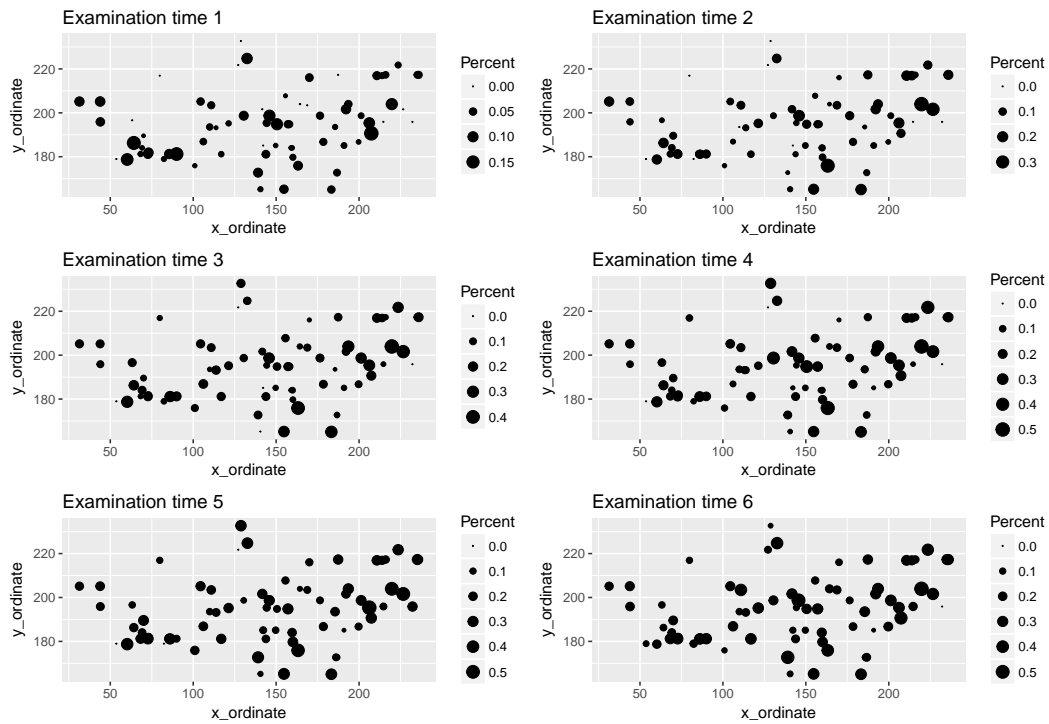


Figure 14: Signal–Tandmobiell[®] data. Apparent prevalence of CE for the different geographical locations of the schools. The results are shown for the different examination times.

Figure 15 shows the spatial distribution of the examiners for the first year of the ST study.

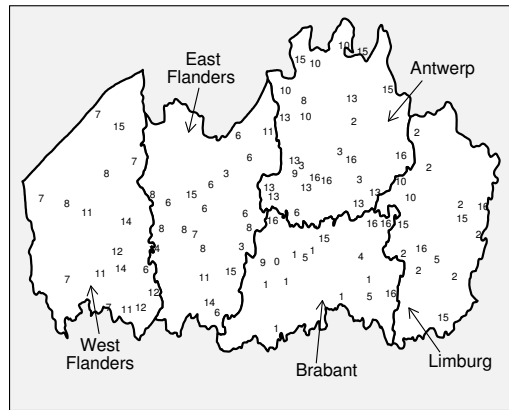


Figure 15: Signal-Tandmobiel[®] data. Spatial distribution of the dental examiners in the first examination year of the study.

Appendix H: Additional results for the Signal-Tandmobiel[®] data

Table 7 shows the observed counts and posterior predictive counts under the different models.

Table 7: Signal-Tandmobiel[®] data. Posterior predicted mean (95% credible interval) for the number of teeth with CE. The results are summarized by tooth and examination (i.e, they correspond to $\sum_{i=1}^N D_{(i,j,k)}$). The results are also presented for different models, along with the observed counts.

Tooth j	Origin of the statistic	Examination					
		1	2	3	4	5	6
1	Observed	40	93	137	182	225	236
	PO	53.91 (37, 71)	92.41 (72, 115)	133.96 (110, 159)	165.99 (141, 192)	210.48 (182, 242)	240.47 (211, 275)
	PO parametric	67.63 (51, 85)	93.05 (72, 113)	124.60 (102, 149)	158.53 (134, 181)	206.37 (179, 234)	247.39 (217, 281)
	PO unstructured correlation	53.16 (38, 68)	90.94 (71, 114)	133.00 (109, 159)	166.35 (139, 197)	208.7 (181, 242)	238.98 (205, 270)
	PH	53.36 (38, 70)	91.60 (70, 114)	132.99 (108, 161)	165.09 (138, 195)	206.96 (175, 243)	239.18 (208, 272)
	AFT	62.08 (44, 79)	94.02 (74, 116)	129.60 (106, 156)	163.66 (135, 194)	207.79 (178, 240)	242.09 (211, 279)
2	Observed	54	100	151	183	229	246
	PO	53.41 (40, 70)	92.33 (74, 113)	134.32 (113, 159)	166.38 (139, 193)	210.20 (183, 240)	240.31(210, 271)
	PO parametric	67.90 (51, 87)	93.22 (74, 114)	125.83 (104, 149)	160.32 (136, 185)	207.94 (180, 235)	248.07 (220, 280)
	PO unstructured correlation	53.65 (39, 71)	91.58 (74, 112)	133.06 (110, 157)	166.52 (142, 191)	209.43 (180, 242)	239.78 (206, 272)
	PH	53.16 (37, 69)	90.85 (72, 111)	132.56 (107, 157)	164.66 (136, 191)	206.12 (175, 235)	238.37 (207, 269)
	AFT	61.85 (45, 80)	94.52 (71, 116)	129.89 (107, 155)	164.20 (138, 192)	207.96 (176, 239)	241.92 (212, 276)
3	Observed	44	93	134	162	208	226
	PO	53.93 (39, 70)	93.12 (71, 114)	134.81 (111, 160)	166.72 (139, 195)	210.33 (182, 244)	241.2 (208, 277)
	PO parametric	67.99 (52, 86)	92.75 (73, 114)	125.38 (102, 147)	159.73 (134, 188)	206.99 (179, 235)	248.44 (216, 282)
	PO unstructured correlation	53.21 (38, 70)	92.47 (74, 113)	133.76 (110, 160)	167.57 (143, 196)	209.43 (181, 240)	240.65 (208, 273)
	PH	53.86 (40, 70)	91.47 (71, 114)	133.68 (109, 158)	165.47 (138, 195)	207.52 (177, 242)	241.01 (210, 278)
	AFT	61.72 (46, 79)	94.45 (75, 116)	130.98 (105, 157)	165.91 (139, 193.)	209.81 (182, 242)	243.18 (214, 275)
4	Observed	47	97	142	177	223	236
	PO	54.06 (38, 70)	92.45 (74, 113)	133.50 (109, 159)	165.59 (139, 196)	209.53 (180, 244)	240.75 (210, 279)
	PO parametric	67.31 (49, 87)	93.31 (74, 115)	125.25 (99, 151)	159.48 (133, 185)	207.12 (176, 235)	247.94 (214, 283)
	PO unstructured correlation	53.80 (39, 70)	92.00 (74, 114)	134.06 (111, 159)	167.41 (142, 197)	209.70 (179, 239)	240.94 (211, 273)
	PH	53.90 (38, 69)	92.11 (69, 113)	133.52 (109, 161)	165.47 (138, 192)	207.42 (174, 238)	240.13 (204, 273)
	AFT	61.70 (43, 80)	94.44 (72.97, 118)	130.64 (105, 156)	164.52 (135, 192)	209.2 (179, 240)	242.83 (212, 278)

Figure 16 shows the posterior predictive mean of the quantile-quantile function for the latent time-to-event residuals under the PO model with a compound symmetry matrix.

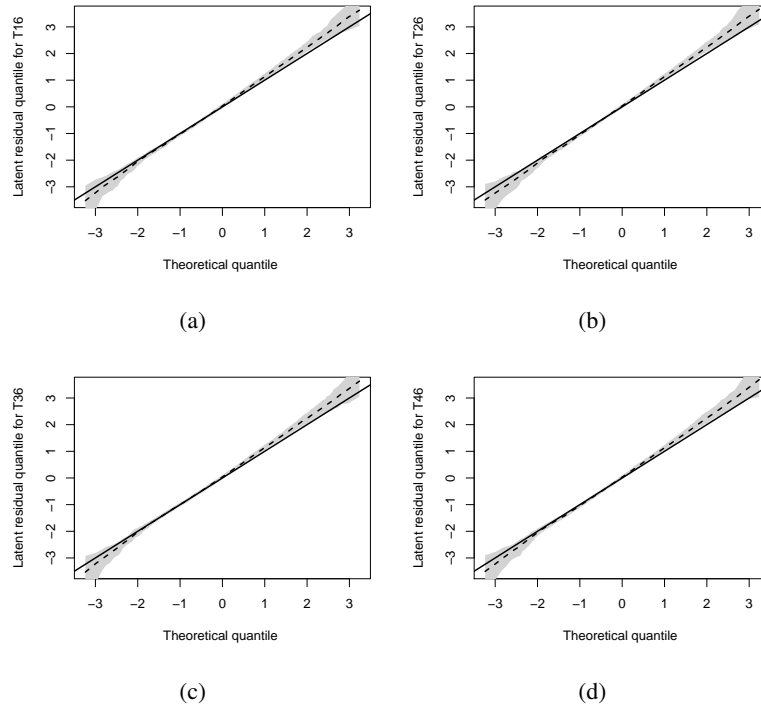


Figure 16: Signal-Tandmobiel[®] data - PO model - compound symmetry matrix: Posterior predictive mean (dotted line) of the quantile-quantile function for the latent time-to-event residuals. The theoretical line is included as a continuous line. A point-wise 95% credible band is displayed as a gray area. The results are shown for the four teeth under consideration.

Figure 17 shows the posterior predictive mean of the quantile-quantile function for the latent time-to-event residuals under the PO model with an unstructured correlation matrix.

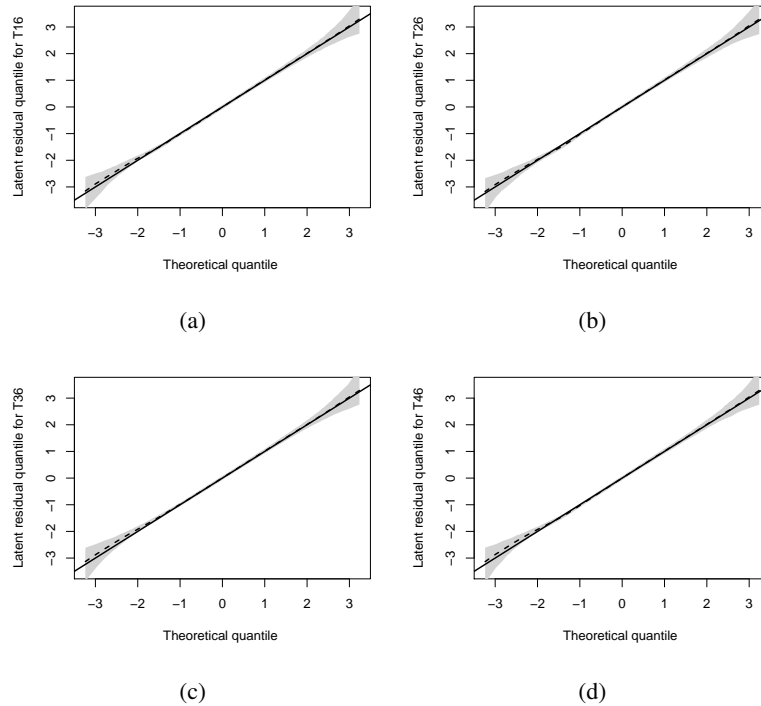


Figure 17: Signal-Tandmobiel[®] data - PO model - unstructured correlation matrix: Posterior predictive mean (dotted line) of the quantile-quantile function for the latent time-to-event residuals. The theoretical line is included as a continuous line. A point-wise 95% credible band is displayed as a gray area. The results are show for the four teeth under consideration.

Table 8 shows the posterior inference for the parameters of marginal time-to-event model. The results are presented for the three versions of the marginal model assuming common β , structured R_ρ , linear terms for x and y and without interaction, and common α and η .

Table 8: Signal-Tandmobiel[®] data. Posterior mean (95% highest posterior density credible interval), for the parameters of marginal time-to-event model. The results are presented for the three versions of the marginal model assuming common β , structured R_ρ , linear terms for x and y and without interaction, and common α and η .

Parameter	Semiparametric Marginal Model		
	PH	AFT	PO
β_1 (Gender; Girl)	0.2269 (0.0382 ; 0.4105)	0.0664 (0.0015 ; 0.1205)	0.2853 (0.0677 ; 0.5049)
β_2 (Age at baseline; years)	0.1920 (0.1094 ; 0.2747)	0.0237 (-0.0045 ; 0.0618)	0.2275 (0.1343 ; 0.3266)
β_3 (Age when brushing starts; years)	-0.3051 (-0.4548 ; -0.1487)	-0.0905 (-0.1400 ; -0.0493)	-0.3108 (-0.5082 ; -0.1202)
β_4 (In between-meal snacks; ≥ 2 a day)	0.14466 (-0.0543 ; 0.3380)	0.0274 (-0.0191 ; 0.0715)	0.1609 (-0.0718 ; 0.4039)
β_5 (x -coordinate)	1.0200 (-0.6345 ; 2.9233)	0.1868 (-0.2995 ; 0.5960)	1.2029 (-0.9065 ; 3.2985)
β_6 (y -coordinate)	-7.2687 (-12.8360 ; -1.7167)	-3.6118 (-5.0231 ; -1.9337)	-8.5588 (-14.7564 ; -2.7341)
ρ	0.6994 (0.6613 ; 0.7399)	0.7142 (0.6761 ; 0.7537)	0.6935 (0.6520 ; 0.7309)

Figure 18 display the posterior predictive mean of the survival function under the selected model and under a semiparametric PO model neglecting the misclassification process. The pointwise 95% credible band under the selected model is displayed as a gray area.

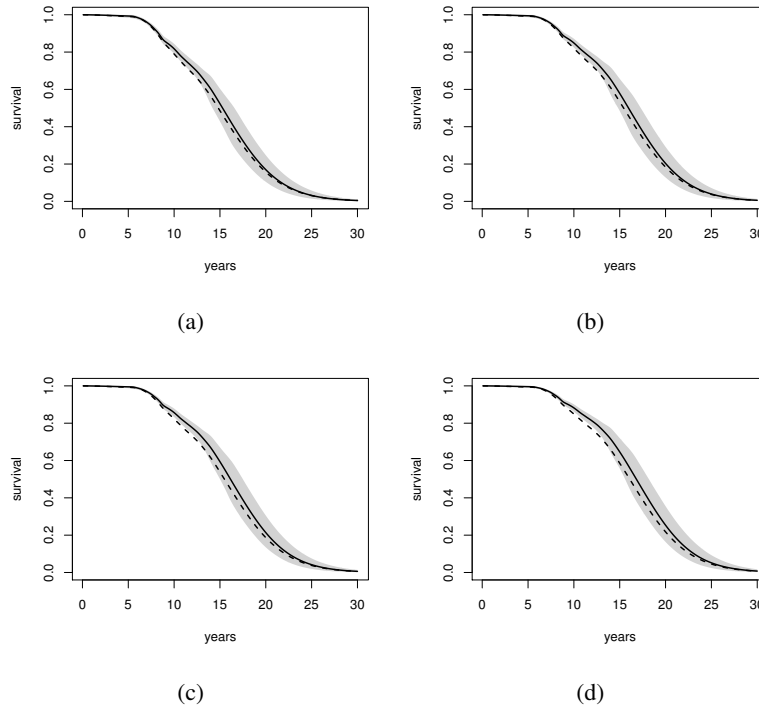


Figure 18: Signal-Tandmobiel[®] data - PO model - misclassification. Posterior predictive mean of the survival function under the selected model (solid line) and under a semiparametric PO model neglecting the misclassification process (dashed line). The pointwise 95% credible band under the selected model is displayed as a gray area. Panel (a) displays the results for a girl, 7.2 years old at baseline, 3 years old when brushing starts, having two or fewer snacks in-between meals, and sample mean x - and y -coordinates. Panel (b) displays the results for a girl, 7.2 years old at baseline, 2 years old when brushing starts, having two or fewer snacks in-between meals, and sample mean x - and y -coordinates. Panel (c) displays the results for a boy, 7.2 years old at baseline, 3 years old when brushing starts, having two or fewer snacks in-between meals, and sample mean x - and y -coordinates. Panel (d) displays the results for a boy, 7.2 years old at baseline, 2 years old when brushing starts, having two or fewer snacks in-between meals, and sample mean x - and y -coordinates.

Figure 19 display the posterior predictive mean of the survival function under the selected model and under a Weibull parametric PO model. The pointwise 95% credible band under the selected model is displayed as a gray area.

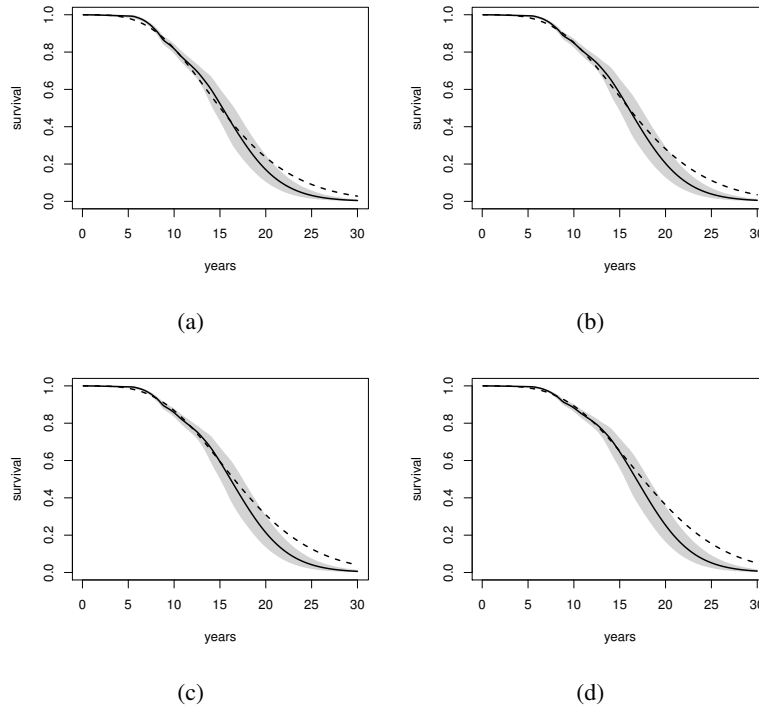


Figure 19: Signal-Tandmobiel[®] data - PO model - nonparametric. Posterior predictive mean of the survival function under the selected model (solid line) and under a Weibull parametric PO model (dashed line). The pointwise 95% credible band under the selected model is displayed as a gray area. Panel (a) displays the results for a girl, 7.2 years old at baseline, 3 years old when brushing starts, having two or fewer snacks in-between meals, and sample mean x - and y -coordinates. Panel (b) displays the results for a girl, 7.2 years old at baseline, 2 years old when brushing starts, having two or fewer snacks in-between meals, and sample mean x - and y -coordinates. Panel (c) displays the results for a boy, 7.2 years old at baseline, 3 years old when brushing starts, having two or fewer snacks in-between meals, and sample mean x - and y -coordinates. Panel (d) displays the results for a boy, 7.2 years old at baseline, 2 years old when brushing starts, having two or fewer snacks in-between meals, and sample mean x - and y -coordinates.

Acknowledgements

The research time of Li was supported in part by the National Cancer Institute grant (5P30CA118100-11; the National Cancer Institute, USA; PI: Willman). The second author was supported by Fondecyt 1141193 and 1180640 grants. The third author was supported by Fondecyt 11110033 grant. The work was partially performed during a visit of the fourth author to Pontificia Universidad Católica de Chile, supported by Fondecyt 11110033 grant. The Signal-Tandmobiel[®] study comprises following partners: D. Declerck (Dental School, Catholic University Leuven), L. Martens (Dental School, University Ghent), J. Vanobbergen (Dental School, University Ghent), P. Bottenberg (Dental School, University Brussels), E. Lesaffre (L-BioStat, Catholic University Leuven) and K. Hoppenbrouwers (Youth Health Department, Catholic University Leuven; Flemish Association for Youth Health Care). The authors thank Sofía and Josefa Jara for proofreading.

References

- Chen, Y.Q., and Jewell, N.P. (2001). On a general class of semiparametric hazards regression models. *Biometrika*, 88(3): 687–702.
- Genz, A. (1992). Numerical computation of multivariate normal probabilities. *Journal of computational and graphical statistics*, 1, 141–149.
- Haario, H., Saksman, E. and Tamminen, J. (2001). An adaptive Metropolis algorithm. *Bernoulli*, 7, 223–242.
- Li, L., Hanson T., and Zhang, J. (2015). Spatial extended hazard model with application to prostate cancer survival. *Biometrics*, 71: 313–322.
- Liu, X., and Daniels, M. J. (2006). A new algorithm for simulating a correlation matrix based on parameter expansion and reparameterization. *Journal of Computational and Graphical Statistics*, 15, 897–914.